Modulated Surface-Plasmon Resonance for *In Situ* Metal-Film Surface Studies

Willes H. Weber
Research Staff, Ford Motor Company, Dearborn, Michigan 48121

(Received 4 April 1977)

A new experimental technique, angle-of-incidence modulated surface plasmon resonance, is used for *in situ* studies on noble-metal films. The method is used to record the real and imaginary parts of the surface-plasmon wave vector and the strength of the surface roughness scattering during room-temperature O_2 exposure. The atomic susceptibility of oxygen on Cu at 632.8 nm is found to be $\chi_a = (1.2 + 1.6i) \times 10^{-24}$ cm^3. Roughly 0.2% of a monolayer can be detected.

Since the first demonstration of optical surface plasmon resonance (SPR) by Otto,[1] the method has been used to study optical constants,[2-6] surface roughness,[7-12] and thin overlayers,[13-15] and to enhance second-harmonic generation[16] and Raman scattering.[17] In this Letter I describe *in situ* experiments on clean and oxygen-covered noble-metal films. The resonances are excited at fixed frequency and variable angle of incidence with a prism coupler in the Kretschmann configuration[4,18] and are detected by the scattered-light method. An angular modulation technique is introduced which increases the sensitivity of the method and allows the direct recording of the real and imaginary parts of the surface-plasmon (SP) propagation vector as well as the strength of the surface roughness scattering. This technique can detect a fraction of a monolayer of an adsorbed gas (e.g., roughly 0.2% of an atomic monolayer of oxygen on Cu can be detected with a signal-to-noise ratio of 1 using a 1-s time constant) or very small changes in the metal optical constants [e.g., a part in 10^4 for Re(ϵ), equivalent to a normal-incidence reflectivity change of 10^{-5}].

SPR is applicable to highly reflecting metal films in a limited frequency regime. Within these limitations, however, it is a high-Q phenomenon ($Q \simeq 10^2$–10^3) and the fields are peaked at the metal surface; thus, its surface sensitivity is enhanced compared with that of more conventional optical measurements. Furthermore, changes in surface roughness can be measured and both the real and imaginary parts of the optical response of an adsorbed molecule can be determined with good precision. These features make SPR complementary to other surface optical techniques such as ellipsometry[19-22] and surface reflectance spectroscopy.[23]

The experiments are done on films grown in a bakable stainless-steel chamber, mounted on a motor-driven rotating table. An optical window serves as the film substrate and another window, opposite it, as the viewing port. Two liquid-N_2 traps separate the chamber from the vacuum pump. After bakeout at ≃300–350°C for 30 h, the pressure reaches $(3-4)\times 10^{-8}$ Torr. Films are evaporated at rates of 1–4 nm/s from either a W or Ta filament, wound in a circular shape and positioned concentric with a line joining the centers of the two windows. A small annular disk screens the viewing window from the filament, at the same time allowing an unobstructed view of the sample. Film thicknesses are 70–90 nm and are measured during growth to ±5 nm. The stability of the film optical measurements for several days after growth indicates that the pressure of adsorbable gases is several orders of magnitude below the ion-gauge pressure.

To excite the resonances a p-polarized, He-Ne laser beam is incident on the film from inside a 45° prism (refractive index $n = 1.51434 \pm 0.0002$), which is coupled to the outside of the sample window with an index-matching oil. A fiber-optic cable connected to a photomultiplier sees the film-vacuum interface from the viewing port. Thus, all optical components are exterior to the chamber and the incident beam enters the vacuum only through the evanescent tail of the surface plasmon.

The resonance curve has a Lorentzian form[4-6]:

$$I = A|(\omega/c)n\sin\theta - \beta|^{-2}, \tag{1}$$

where I is the intensity of scattered light, θ is the angle of incidence in the prism, β is the complex SP propagation vector, and A is the product of the nonresonant part of the transmission factors describing the SP excitation and a factor describing the surface roughness scattering which couples the light out. The measurement of $I(\theta)$ thus determines the complex SP propagation vector. The peak position θ_m and half-width at half-maximum $\Delta\theta$ give, respectively, the real and imaginary parts of β:

$$\mathrm{Re}(\beta) = (\omega/c)n\sin\theta_m, \qquad \mathrm{Im}(\beta) = (\omega/c)n\cos\theta_m\Delta\theta. \tag{2}$$

In the following we refer to the experimentally recorded angle of incidence α on the prism entrance face, which is related to θ by $n\sin(\theta-\gamma)=\sin\alpha$, where γ is the prism angle. Note that small changes in α_m and $\Delta\alpha$ are proportional to small changes in θ_m and $\Delta\theta$, respectively.

The angle α is modulated at $f\simeq 400$ Hz with a peak-to-peak amplitude of 0.1–0.2°. This is achieved by reflecting the beam off a small, angularly vibrating mirror which scans the beam across a lens positioned to reimage it onto the sample. In this way the beam remains fixed on the sample while α is varied. The modulated signal on the photomultiplier at f gives $dI/d\alpha$, while the signal at $2f$ gives $d^2I/d\alpha^2$. Figure 1 shows an example of a normal resonance curve and first and second derivatives obtained on a clean Cu film. On resonance, $\alpha=\alpha_m$, one can readily show that

$$I\propto A(\Delta\alpha)^{-2},\ dI/d\alpha=0,\ d^2I/\alpha^2\propto A(\Delta\alpha)^{-4}. \tag{3}$$

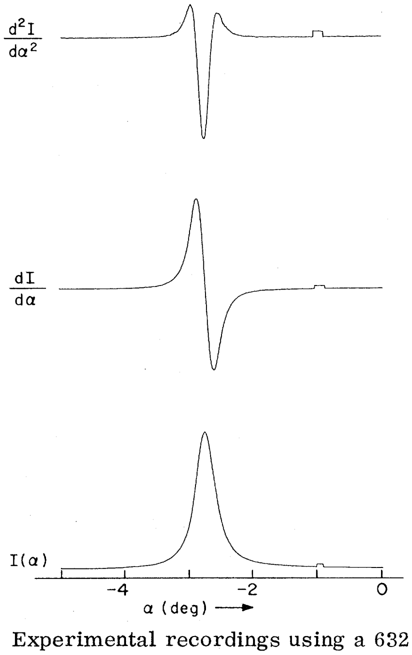

FIG. 1. Experimental recordings using a 632.8-nm HeNe laser of surface-plasmon resonance on a 84-nm Cu film 2 days after growth. Experimental conditions are 1°/m scan rate, 0.1 s time constant, and 0.13° peak-to-peak angular modulation for the derivative curves. The marks near $\alpha=-1°$ are for angular calibration.

When a surface is exposed to an adsorbing gas, the position and width of the resonance may change, as well as the surface roughness scattering. To record these changes versus time after exposure, a servo-mechanical system is employed to keep $dI/d\alpha=0$ by driving the rotating table. Thus the angle of incidence stays "tuned" to the resonance, and the quantities α_m, $I(\alpha_m)$, and $d^2I(\alpha_m)/d\alpha^2$ can be directly recorded. With a variable-frequency light source, the same procedure could be used to record a SP spectrum.

An example of the data obtained using this method is shown in Fig. 2 for a Cu film exposed to O_2. At $t=0$ a small measured quantity of O_2 is released into the chamber. The signals change rapidly at first and then stabilize after 40–50 s, since all the O_2 has been gettered by the Cu. From the known Cu surface area, I estimate the coverage at this point to be 1×10^{15} atoms/cm^2. At $t=52$ s a second quantity of O_2 is introduced, roughly 10^3 larger than the first, and again there is an abrupt change in the signals. This time, however, $I(\alpha_m)$ and $d^2I(\alpha_m)/d\alpha^2$ show very little change after the abrupt jump, while α_m shows a continued increase. This increase results from the growth of an oxide layer. The quantity $I^2(\alpha_m)\times[d^2I(\alpha_m)/d\alpha^2]^{-1}$, which is proportional to the surface roughness scattering, remains unchanged during the O_2 exposure. Thus all the effects can be attributed to a shift in the SP propagation vector.

Since the experiments are done on rather thick metal films with very thin overlayers, I treat the overlayer effect as a perturbation to the semi-

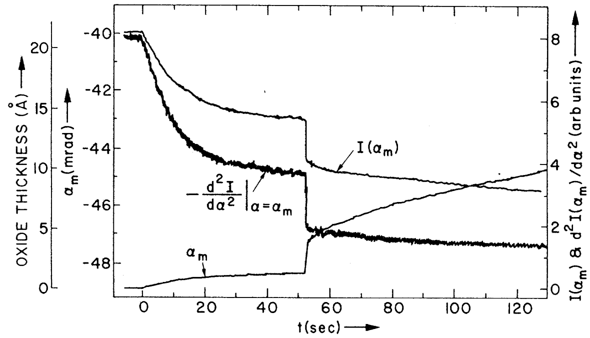

FIG. 2. Simultaneous recordings of α_m, $I(\alpha_m)$, and $d^2I(\alpha_m)/d\alpha^2$ as O_2 is adsorbed onto a clean 82-nm Cu film. At $t=0$, a quantity of O_2 is introduced sufficient to yield $\simeq1\times10^{15}$ atoms/cm^2 on the Cu-coated surfaces. At $t=52$ s a 10^3-larger quantity is introduced; the pressure reaches $\simeq0.1$ Torr and changes very slightly thereafter.

infinite-metal case. With this simplification it follows[24] that the overlayer produces a shift $\delta\theta$ in the SP propagation vector given by

$$\delta\beta=\frac{\omega^2}{c^2\beta}\frac{\epsilon_1\epsilon_3k_1k_3}{(\epsilon_1k_1+\epsilon_3k_3)(\epsilon_1+\epsilon_3)}\times\frac{(\epsilon_2-\epsilon_3)(\epsilon_1-\epsilon_2)d_2}{\epsilon_2}, \qquad (4)$$

where ϵ_1, ϵ_2, and ϵ_3 are, respectively, the dielectric constants of the metal, overlayer, and vacuum; $\beta=(\omega/c)[\epsilon_1\epsilon_3/(\epsilon_1+\epsilon_3)]^{1/2}$ is the SP vector for the metal-vacuum interface; $k_i=(\beta^2-\epsilon_i\omega^2/c^2)^{1/2}$; and d_2 is the overlayer thickness. For a high-Q resonance the real parts of β, ϵ_1, k_1, and k_3 are large compared with their corresponding imaginary parts. Thus, a transparent overlayer will change only $\mathrm{Re}(\beta)$, while a lossy one will change both $\mathrm{Re}(\beta)$ and $\mathrm{Im}(\beta)$.

Equation (4) is not expected to be valid for a submonolayer film, where ϵ_2 and d_2 lose their usual meaning. Although effective ϵ's and d's can be defined for such a film,[25] it can also be treated as a two-dimensional collection of polarizable atoms.[19,21,22] To do this, we set $(\epsilon_2-\epsilon_3)d_2 = n_a 4\pi\chi_a$ in the numerator of Eq. (4) and $\epsilon_2=\epsilon_3$ elsewhere, the result being

$$\delta\beta=\frac{\omega^2}{c^2\beta}\frac{\epsilon_1k_1k_3(\epsilon_1-\epsilon_3)}{(\epsilon_1k_1+\epsilon_3k_3)(\epsilon_1+\epsilon_3)}n_a4\pi\chi_a, \qquad (5)$$

where n_a is the surface density and χ_a the atomic susceptibility of the adsorbed atom for the SP polarization. Equation (5) is an approximate result that is strictly valid only in the low-coverage limit where $\epsilon_2\simeq\epsilon_3$ and Lorentz-Lorenz corrections are unimportant. Furthermore, Feibelman[26] has pointed out that optical constants for surface atoms might not be well defined for p polarization. However, to the extent that $\delta\beta$ is proportional to n_a, one may consider Eq. (5) as a definition for the possibly phenomenological paramater χ_a.

To demonstrate the use of Eqs. (4) and (5), it is is convenient to plot the trajectory of the SP wave vector in the complex β plane as the oxygen coverage increases. Such a plot is equivalent to plotting $\Delta\alpha$ as a function of α_m, since, for small shifts in β, $\delta\beta$ is proportional to $\delta\alpha_m+i\delta(\Delta\alpha)$. Figure 3 shows the data from Fig. 2 analyzed according to Eqs. (3) and replotted in the above manner.

The data at low and high coverages show very different slopes, with the transition between the two occurring at $(1-2)\times10^{15}$ atoms/cm^2. The high-coverage results correspond to an oxide layer, those at low coverage to a chemisorbed oxygen layer. Measurements on several other samples indicate that $\delta\beta\propto n_a$ in the range below 10^{15} cm^{-2} and that the transition between the two regions occurs smoothly as indicated by the dashed line in Fig. 3. By fitting the low-coverage points by a straignt line and using Eq. (5), I estimate the atomic susceptibility to be $\chi_a=(1.2+1.6i)\times10^{-24}$ cm^3. The large imaginary part of χ_a indicates a chemisorbed rather than a physisorbed state. The absolute uncertainty in χ_a is $\simeq 20\%$ due to the coverage uncertainty. Low-energy-electron diffraction measurements[27] on Cu(111) indicate a monolayer structure of oxygen occurring at 300 K for a coverage of 1.2×10^{15} atoms/cm^2, which is within the transition region on Fig. 3. This result is not surprising, since evaporated noble-metal films are expected to have a ⟨111⟩ fiber texture.[28]

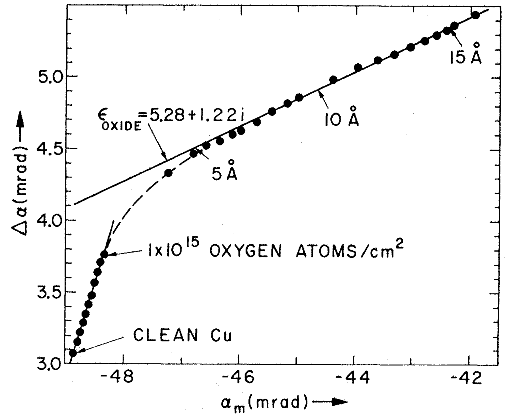

FIG. 3. Plot of $\Delta\alpha$ vs α_m as O_2 adsorbs onto Cu determined from data in Fig. 2. The lower line is drawn using Eq. (5) with $\chi_a=(1.2+1.6i)\times10^{-24}$ cm^3 and $\epsilon_1 = -15.06+0.85i$. The upper line is drawn using Eq. (4) with $\epsilon_2=5.28+1.22i$; the starting point is shifted upward in $\Delta\alpha$ to account for the lossy Cu-oxide interface.

With continued O_2 exposure an oxide layer begins to form. My experiments yield two pieces of data, α_m and $\Delta\alpha$, and these by themselves cannot uniquely determine the three oxide parameters: $\mathrm{Re}(\epsilon_2)$, $\mathrm{Im}(\epsilon_2)$, and d_2. Although there is some question regarding the nature of the oxide which forms, we presume it to be $CuO_{0.67}$, which is a gross defect structure of Cu_2O. Wieder and Czanderna[29] have established that $CuO_{0.67}$ is the oxide formed at room temperature, and they have measured its optical properties.[30] The upper solid line in Fig. 3 is drawn using their $\mathrm{Re}(\epsilon_2)$ value ($=5.28$ at $\lambda=632.8$ nm) in Eq. (4) and adjusting $\mathrm{Im}(\epsilon_2)$ to fit the high-coverage data. The resulting Im(ϵ_2) value is twice as large as that found for their thicker films grown at 110°C.[30] The oxide-thickness scale in Fig. 2 and the markers in Fig. 3 are determined from Eq. (4). These thicknesses are, of course, not meaningful below a few angstroms. The oxidized surface appears as a relatively transparent oxide on top of a highly absorbing Cu-oxide interface. It is significant that the extrapolation of the oxidized-surface data to zero oxide thickness does not yield the result for a clean Cu surface. Beyond the transition region, the thickness varies with time as $d \propto \mathrm{const} + \ln t$. This dependence is consistent with the growth being limited by diffusion of Cu vacancies through the oxide, which is the expected rate-limiting mechanism.[31]

On both Ag and Au films the oxygen adsorption saturates and no thick oxide forms. The actual coverage is more uncertain on these films than it is on Cu, since the O_2 sticking coefficient is much smaller on Ag and Au.[32] However, the shifts in Re(β) after saturation can be explained using Eq. (5) with the molecular susceptibility of O_2 at 632.8 nm, determined from the refractive index of liquid O_2, and assuming a coverage of one oxygen atom per metal atom. Both Re(β) and Im(β) change with O_2 adsorption on Ag, suggesting a chemisorbed state, but only Re(β) changes significantly with O_2 on Au.

I would like to thank B. Poindexter for his expert assistance in building the apparatus and for recording much of the data.

---

[1] A. Otto, Z. Phys. 216, 398 (1968).

[2] A. S. Barker, Jr., Phys. Rev. Lett. 28, 5418 (1972), and Phys. Rev. B 8, 5418 (1973).

[3] E. Kretschmann, Z. Phys. 241, 313 (1971).

[4] R. Bruns and H. Raether, Z. Phys. 237, 98 (1970).

[5] W. H. Weber and S. L. McCarthy, Appl. Phys. Lett. 25, 396 (1974).

[6] W. H. Weber and S. L. McCarthy, Phys. Rev. B 12, 5643 (1975).

[7] E. Kretschmann, Z. Phys. 227, 412 (1969).

[8] D. Hornauer, H. Kapitza, and H. Raether, J. Phys. D 7, L100 (1974).

[9] E. Kretschmann, Opt. Commun. 10, 353 (1974).

[10] A. J. Braundmeier and E. T. Arakawa, J. Phys. Chem. Solids 35, 517 (1974).

[11] D. L. Mills, Phys. Rev. B 12, 4036 (1975).

[12] H. J. Simon and J. K. Guha, Opt. Commun. 18, 391 (1976).

[13] K. Holst and H. Raether, Opt. Commun. 2, 312 (1970).

[14] F. Abelès and T. Lopez-Rios, in *Proceedings of the First Taormina Research Conference on the Structure of Matter, 1972,* edited by E. Burstein and F. DeMartini (Pergamon, New York, 1974), p. 241.

[15] K. Bhasin, D. Bryan, R. W. Alexander, and R. J. Bell, J. Chem. Phys. 64, 5019 (1976).

[16] H. J. Simon, D. E. Mitchell, and J. G. Watson, Phys. Rev. Lett. 33, 1531 (1974).

[17] Y. J. Chen, W. P. Chen, and E. Burstein, Phys. Rev. Lett. 36, 1207 (1976).

[18] E. Kretschmann and H. Raether, Z. Naturforsch. A23, 2135 (1968).

[19] R. W. Stobie, B. Rao, and M. J. Dignam, Surf. Sci. 56, 334 (1976).

[20] R. C. O'Handley, D. K. Burke, S. N. Jasperson, and E. J. Ashley, Surf. Sci. 50, 407 (1975).

[21] G. A. Bottsma and F. Meyer, Surf. Sci. 13, 110 (1969).

[22] T. Smith, J. Opt. Soc. Am. 58, 1069 (1968).

[23] G. W. Rubloff, J. Anderson, M. A. Passler, and P. J. Stiles, Phys. Rev. Lett. 32, 667 (1974), and Phys. Rev. B 10, 2401 (1974).

[24] This result follows from the location of the pole for a complex angle of incidence in the three-media, *p*-polarized, Fresnel transmission coefficient.

[25] J. D. E. McIntyre, Surf. Sci. 37, 658 (1973).

[26] P. J. Feibelman, Phys. Rev. B 14, 762 (1976).

[27] G. W. Simmons, D. F. Mitchell, and K. R. Lawless, Surf. Sci. 8, 130 (1967).

[28] See, for example, K. L. Chopra, *Thin Film Phenomena* (McGraw-Hill, New York, 1969), pp. 220–221.

[29] H. Wieder and A. W. Czanderna, J. Phys. Chem. 66, 816 (1962).

[30] H. Wieder and A. W. Czanderna, J. Appl. Phys. 37, 184 (1966).

[31] T. N. Rhodin, J. Am. Chem. Soc. 72, 5102 (1950).

[32] A. W. Dweydari and C. H. B. Mee, Phys. Status Solidi (a) 17, 247 (1973).